

Metal-supported solid oxide fuel cell membranes for rapid thermal cycling

Yuriy B. Matus^{a,b}, Lutgard C. De Jonghe^{b,*}, Craig P. Jacobson^b, Steven J. Visco^b

^aDepartment of Materials Science and Engineering, University of California at Berkeley, Berkeley, CA 94720, United States

^bMaterials Sciences Division, Lawrence Berkeley National Laboratory Berkeley, 1 Cyclotron Road build 62/245 CA 94720, United States

Received 14 January 2004; received in revised form 3 September 2004; accepted 17 September 2004

Abstract

Solid oxide fuel cell (SOFC) membranes were developed in which zirconia-based electrolyte thin films were supported by a porous composite metal/ceramic current collector and were subjected to rapid thermal cycling between 475 and 1075 K (200 and 800 °C). The effects of this cycling on membrane performance were evaluated. The membranes, not yet optimized for performance, showed a peak power density of 350 mW/cm² at 1175 K (900 °C) in laboratory-sized SOFCs, while rapid thermal cycling had only a marginal effect on cell performance. This resistance to cycling degradation is attributed to the close matching of thermal expansion coefficient of the porous cermet supporting current collector (PCC) with that of the zirconia electrolyte.
Published by Elsevier B.V.

Keywords: Thin film SOFC; Metal support electrodes; Thermal cycling; Fast response

1. Introduction

An essential characteristic of solid oxide fuel cell (SOFC) membranes designed for distributed standby power or for auxiliary power units (APUs) is their ability to withstand rapid thermal cycles. A first requirement of such fuel cell systems is a sufficient power density at intermediate operating temperatures. A second requirement is that the membrane materials be compatible, both during fabrication and during use. A third requirement is that such fuel cell systems can be brought into operation rapidly from ambient temperatures, preferably in a matter of minutes. Economic considerations also impose the use of intrinsically low-cost materials. Numerous authors have reported meeting the power requirements at reduced temperatures through the use of anode-supported thin film solid oxide fuel cell membrane [1–9].

The requirement of significant cost reduction, as well as robustness of the membranes, has prompted the exploration

of alternative membrane architectures in which the structural and the catalytic functions of the supporting porous electrode are separated. In the past, cheap steel alloys have been used only as current interconnects [10,11]. In our new configuration, a porous metallic alloy provides the mechanical support for the electrolyte film and serves as the electrical connection, while the electrocatalytic function is maintained by a thin (10–15 μm) layer of Ni/zirconia at the solid electrolyte/porous steel alloy interface [12,13]. In this paper, the porous cermet current collector will be referred to as the PCC.

A remaining issue—particularly important in the context of intermittently operating systems—is the capability of the fuel cells to withstand not only repeated [14–16] but also rapid thermal cycling. There are, as yet, no fully satisfactory answers to reliability questions for solid oxide fuel cells in intermittent distributed power scenarios. The basic problem is one of materials compatibility. The present work seeks to remedy this problem through the identification and evaluation of metal alloy/ceramic (cermet) materials that can support a thin film solid oxide electrolyte, without causing failure of the SOFC membrane during rapid thermal cycling, while also serving as a current collector.

* Corresponding author. Tel.: +1 510 486 6138; fax: +1 510 486 4881.

E-mail address: LCDejonghe@lbl.gov (L.C. De Jonghe).

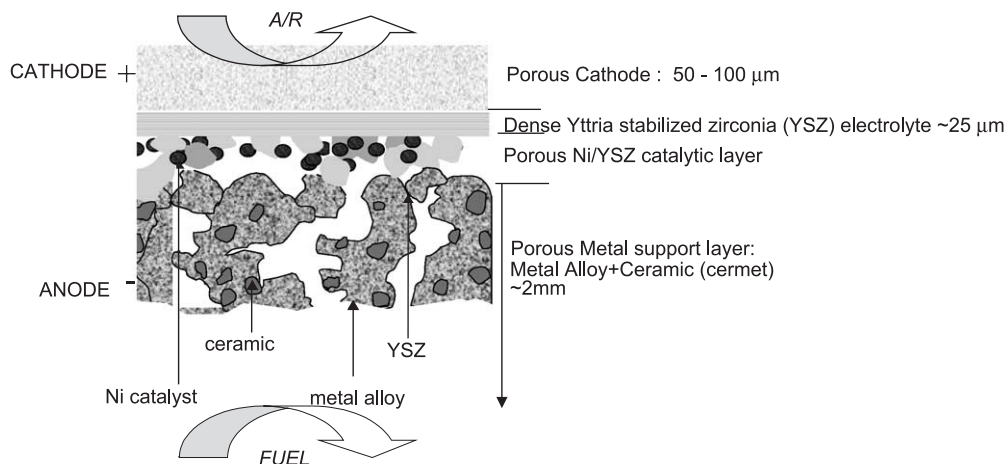


Fig. 1. General architecture of the multilayered fuel cell membrane.

A thin ceramic electrolyte film (10–30 μm) is essential for lowering the operating temperature of SOFCs from the usual ~ 1275 to 925 – 1075 K (650 – 800 $^{\circ}\text{C}$). Reduction of the operating temperatures to below 1075 K offers the possibility of using metallic interconnects without their excessive oxidation, while still allowing for direct reforming of hydrocarbons, and for some practical forms of cogeneration. In a typical SOFC membrane configuration, a porous composite Ni/yttria stabilized zirconia (YSZ) anode, 1 to 2 mm thick, supports the zirconia-based electrolyte film. However, this Ni/YSZ anode layer can add significant cost due to its needed high-volume fraction of zirconia. In addition, the Ni/YSZ electrode is mechanically rather fragile. Employing ferritic FeCr alloys as the major mechanical support for the SOFC membrane not only reduces materials costs significantly, but also adds greatly to the mechanical robustness of the membrane. While the thermal expansion of these alloys can be close to that of the yttria or scandia-doped zirconia electrolyte, a complete match is necessary for rapid thermal cycling. This matching was achieved by dispersing a compatible, low thermal expansion ceramic into the FeCr alloy to form the supporting PCC.

The SOFC multilayered membrane must also satisfy chemical compatibility of the various functional layers and reach sufficient area-specific power density. Electrodes must have high electronic conductivity and appropriate, stable porosity to minimize Ohmic and mass transport overpotentials. To meet those requirements metal-supported multilayered SOFC membranes with the general architecture shown in Fig. 1 were produced and tested. The response to extensive rapid thermal cycling of these membranes was evaluated in a fuel cell configuration, before and after thermal cycling at approximate rate of 50 K/min between 475 and 1075 K. Such cooling and heating rates are actually more severe than could reasonably be expected in distributed power generation scenarios but approach the requirements for APUs (50 – 100 K/min).

2. Experimental

2.1. Synthesis of starting materials

To minimize the ceramic content of the ferritic alloy used here, i.e., FeCr containing 30 wt.% chromium (Fe30Cr), addition of a near-zero coefficient of thermal expansion (CTE) material would be ideal. A candidate material was aluminum iron titanate (AFT, $\text{Al}_{1.57}\text{Fe}_{0.43}\text{TiO}_5$) with a CTE of less than $0.2 \times 10^{-6} \text{ K}^{-1}$ [17,18]. Assuming a simple rule of mixtures, only 5 vol.% of ATF would be needed to produce a cermet that fully matches the CTE of an 8YSZ electrolyte. In contrast, a complete CTE match through addition of alumina (CTE $\sim 8.5 \times 10^{-6} \text{ K}^{-1}$) would require as much as 30 vol.% of this ceramic, adversely affecting electronic conductivity and increasing brittleness. However, AFT is unstable in the reducing atmospheres necessary for the cofiring process used here to make the SOFC membranes, decomposing into aluminum titanate (AT) and iron. Aluminum titanate was therefore chosen as the ceramic additive. AT also has a very low CTE ($\sim 0.5 \times 10^{-6} \text{ K}^{-1}$) [19]. To match the thermal expansion of the YSZ by using AT rather than AFT in the Fe30Cr alloy, the amount of ceramic additive needed to be increased from 5% to only 6% by volume (~ 3 wt.%).

Two different routes were followed to prepare the AT compound. A first route was by a solid-state reaction between alumina and titania¹. The component oxide powders were mixed in the appropriate proportions (50.1, 49.9 of Al_2O_3 , TiO_2 by weight percent, respectively), milled together in acetone in an attritor mill, and calcined at 1300 $^{\circ}\text{C}$ in an oxidizing atmosphere. This AT powder was remilled in an attritor mill, in acetone, for 3 h at 550 rpm. Subsequently, the AT powder was dried under a heat lamp, passed through a 25 - μm sieve, and mixed with Fe30Cr

¹ Compositions including iron oxides having a lower CTE than AT were also evaluated but proved to be unstable to reduction.

powder with a particle diameter between 38 and 75 μm to make the Fe₃₀Cr₃AT cermet, i.e., Fe₃₀Cr containing 3 wt.% of AT. 2.54×10^{-2} m (1 in.) diameter disks were prepared from this cermet powder by die-pressing at 0.689 MPa (10,000 psi) and firing at 1625 K in a reducing atmosphere.

A second method for preparing the low-expansion additive was a sol–gel process. The gel was prepared from titanium butoxide (Aldrich Chemical) and aluminum nitrate (Alfa Aesar; 1:1 by weight Al nitrate and Ti butoxide). Five grams of the solids was mixed into 20 ml isopropanol, in a nitrogen-protective environment. Seven drops of ammonia, diluted in deionized water 1:3 by volume, were added to the Al nitrate, Ti butoxide with isopropanol mixture and vigorously mixed for 5 min. The sol was then mixed with the Fe₃₀Cr alloy powder and dried under a heat lamp for 6 h, completing the sol–gel transformation.

2.2. Fabrication of the porous cermet supporting current collector (PCC)

The porous Fe₃₀Cr₃AT cermet support layers were fabricated following two different processing methods. Method A included a prefiring of the porous cermet layers in a reducing atmosphere, while method B involved a prefiring in an oxidizing atmosphere (ambient air). The method of addition of the AT was the same in method A and B. In contrast to the sol–gel-prepared AT, addition of the solid-state-prepared AT did not lead to a satisfactory distribution of this low-expansion additive and was not pursued further.

2.2.1. Method A

Fe₃₀Cr₃AT powder was mixed with 3 wt.% Carbowax binder dissolved in isopropanol (1 g Carbowax in 20 ml of isopropanol). The slurry then was dried under a heat lamp for 4 h at 395 K (120 °C). The dried powder was passed through a 100- μm sieve with opening and die-pressed at 0.689 MPa (10,000 psi) in a 1-in. diameter steel die to form the support layer of the SOFC membrane. The pressed disks were prefired in a reducing atmosphere of 4% H₂ in Argon at 1175 K for 2 h. This prefiring gave enough strength to the cermet for the subsequent manipulations involved in the integration of the additional functional layers (shown in Fig. 1).

2.2.2. Method B

The Fe₃₀Cr₃AT powder was mixed with 5 wt.% stearic acid dissolved in acetone binder by weight and dried under a heat lamp for 20 min at 80 °C. The dried powder was sieved through a 100- μm sieve and die-pressed into the 2.5×10^{-2} m (1 in.) diameter disks at 6.9×10^5 Pa (10,000 psi). The disks were prefired in oxidizing atmosphere at 675 K. This low-temperature prefiring step in oxidizing atmosphere gave sufficient strength to the disks, similar to the one obtained in method A. In this case, the strength of the disk was due to the low-temperature oxide formation, bonding the metal

particles. Surface oxidation of these prefired metal disks was evidenced by their discoloration, attributed to the formation of chromium oxide and iron oxides.

2.3. Integration of Ni/YSZ catalytic layer

The porous Ni/YSZ catalyst layer was deposited on the prefired Fe₃₀Cr₃AT cermet support electrode, either by modified tape casting or by screen printing. Mixtures of YSZ and NiO (45 and 45 wt.%), polyvinyl butyral (PVB), and polyethylene glycol (5 and 5 wt.%) were suspended together in the isopropanol and milled in an attritor mill for 3 h at 550 rpm. Then, the attritor-milled slurry used for the NiO/YSZ layer was applied by either tape casting or screen printing, and the samples were prefired at 775 K in ambient atmosphere to achieve binder burnout, leaving an adherent, porous NiO/YSZ layer. The surface of the deposited NiO/YSZ layer was smooth and showed no visible flaws at 200 \times magnification. For high substrate porosities, it was necessary to increase the NiO/YSZ slurry viscosity by increasing solids loading until the slurry no longer penetrated the porous substrate, forming a smooth layer on which the electrolyte layer would be deposited.

2.4. Application of the YSZ electrolyte film

The YSZ electrolyte film was applied following three different methods: tape casting, vacuum infiltration of a colloidal suspension, or colloidal spray deposition. Tape casting of the YSZ film was similar to the application of the Ni/YSZ catalytic layer. However, the densification and thickness of the electrolyte deposited by tape casting were inferior to that of the other two techniques.

The vacuum infiltration setup is shown schematically in Fig. 2. The colloidal suspension consisted of 0.8 g/l of YSZ powder (Tosoh), with an average diameter of 0.35 μm , suspended in isopropanol by ultrasonication for 4 min. The substrate (porous Fe₃₀Cr₃AT cermet disc with the prefired Ni/YSZ catalytic layer) was affixed to the vacuum line and immersed into the YSZ colloidal suspension, as shown in Fig. 2. Both the suspension concentration and the immersion time, typically 5 min, determined the thickness of the colloidal YSZ deposit. The process in some respects resembles slip casting, but the suspension is much less concentrated compared to regular slip casting. High solids loading in colloidal vacuum infiltration make the control of the deposit thickness very difficult and is thus to be avoided. To manage shrinkage of the YSZ electrolyte, the green density of the deposited film needs to be carefully controlled. The density of the as-deposited YSZ layer was affected by the nature of the solvent. YSZ suspensions in alcohol led to at least 3% less film linear shrinkage compared to water-based suspensions. However, the water-based process required very slow drying (as much as 5 h at room temperature) to avoid film drying cracks. The vacuum infiltration technique requires the surface of the

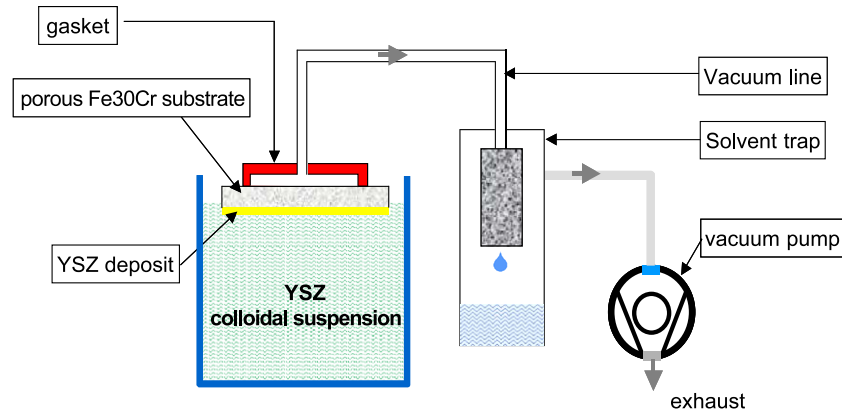


Fig. 2. Schematic for YSZ vacuum infiltration deposition.

porous substrate layer to be highly uniform, with substrate pores no larger than about three to five times the powder agglomerate diameter. Additionally, accidental inclusion of organic or inorganic dust particles may introduce pinholes in the sintered electrolyte and must be avoided. Increasing the thickness of the YSZ film can in part compensate for the deleterious presence of larger pores or other imperfections exceeding this tolerance, but this leads to an excessive electrolyte resistance.

For colloidal spray deposition, YSZ powder (Tosoh) was suspended in isopropanol at 5 g/l. Spray-deposited green film properties could be modified by binder addition (PVB or Carbowax binders). Addition of 10 to 20 vol.% of binder increases the strength of the green film, making it potentially possible to build thicker YSZ electrolyte films without the cracks that otherwise could develop due to excessive drying stresses. However, suspension modification by such binder addition invariably led to agglomerate formation and was not a successful strategy for obtaining continuous thin green films. For spray deposition, YSZ/isopropanol suspensions without binder altogether yielded the best, smooth, and flawless green films. After cofiring of the multilayer SOFC membrane at

1625 K (1350 °C), in reducing atmosphere, for 4 h, the resulting YSZ electrolyte film was dense and free of pinholes and electronic shorts.

Vacuum infiltration and spraying depositions led to a similar quality of electrolyte films, but spraying was a more convenient technique for the lab-prepared SOFC.

The sintered membranes were sealed onto an alumina tube with Ceramabond 571-p and Ultra-Temp-516 sealing compounds from Aremco Products. Subsequently, $\text{La}_{0.6}\text{Sr}_{0.4}\text{Co}_{0.8}\text{FeO}_3$ (LSCF), prepared by the Glycine Nitrate Process (GNP) described elsewhere [20], was used for producing functioning cathodes. The cathode was sprayed onto the YSZ electrolyte of the cofired membrane and sintered at 1175 K. Pt mesh, serving as a current collect, was subsequently attached with Pt paste to the sintered cathode, and bonding was achieved by heating to 1175 K.

2.5. Electrochemical testing

Current–voltage (I – V) data for the Fe30Cr3AT-supported cells were collected on 2.54×10^{-2} m (1 in.) diameter button cells with a cathode active area of 2.5×10^{-5} m², using a Princeton Applied Research potentiostat Model 371, at a current-increment rate of 15 mA/min. In addition, the AC

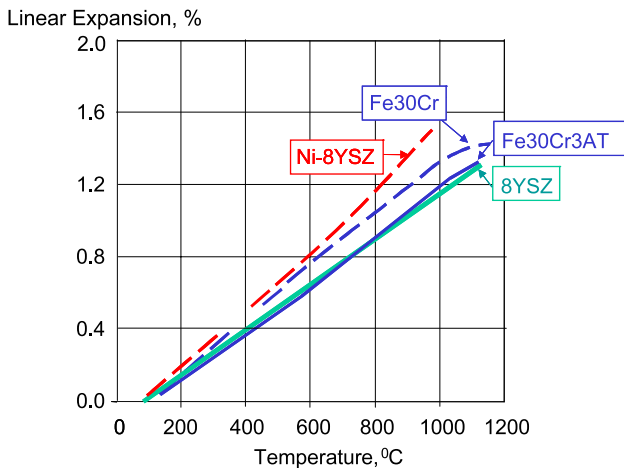


Fig. 3. Thermal expansion of 8YSZ electrolyte, Ni/8YSZ anode, Fe30Cr alloy, and Fe30Cr3AT.

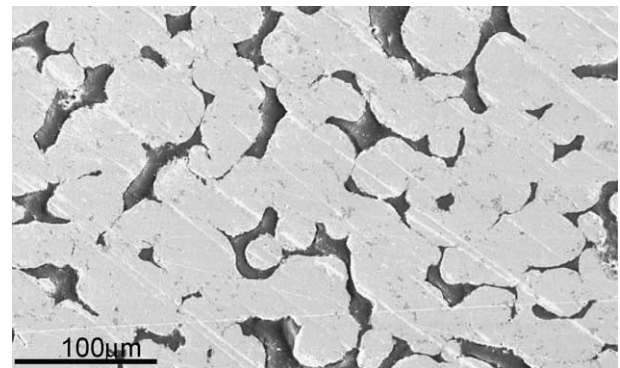


Fig. 4. Scanning electron microscope image of a polished cross-section of the cermet support. Distributed particles of AT may be discerned. The dark areas are the mounting epoxy needed to allow polishing.

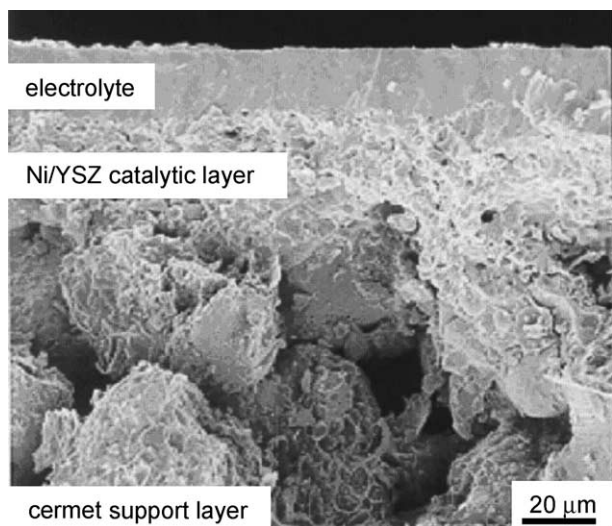


Fig. 5. Fracture cross-section of Fe₃₀Cr₃AT-supported SOFC electrolyte layer after cofiring at 1625 K before thermal cycling. The cermet support layer (PPC) shows large pores, as well as features typical of some plastic deformation that resulted when fracturing the multilayer membrane.

impedance was also recorded, showing results in agreement with I – V characteristics.

3. Results and discussion

3.1. Thermal expansion measurements

To determine the thermal expansion of YSZ, Ni/YSZ, Fe₃₀Cr, and Fe₃₀Cr₃AT, dilatometer measurements were made. Pellets (4×10^{-3} m diameter and 2.54×10^{-2} m thick) of the various powders were die-pressed at 0.689 MPa and heated in an Orton dilatometer (Model 1600). The thermal expansion of the AT was negligible compared to that of the Fe₃₀Cr alloy. The thermal expansion of the materials was recorded between room temperature and 1475 K and is shown in Fig. 3.

The dilatometer studies showed that thermal expansion of the metal/ceramic composite substrate was matched fully with that of the 8YSZ electrolyte.

3.2. PCC layer microstructure

The low-CTE additive distribution in the metal substrate and microstructure of the fuel cell support were studied using SEM. The porous metal support layer prepared by sol-gel incorporation of AT (alumina titanate) into the Fe₃₀Cr powders showed a uniform distribution of the near-zero thermal expansion compound between the ferritic alloy grains as shown in Fig. 4.

Attempts to use La_{0.65}Sr_{0.35}MnO₃ (LSM) as a cathode in the cofired structure were not successful. LSM is not stable in reducing atmosphere needed for cofiring. Moreover, attempts to form LSM cathodes in situ during the heat-up of the SOFC test rig did not lead to a usable cathode. In contrast, La_{0.6}Sr_{0.4}Co_{0.8}FeO₃ (LSCF) sinters at lower temperature and these cathodes could be fired-on at 1175 K for 1 h. Cross-sections of complete Fe₃₀Cr₃AT-supported fuel cell membranes are shown in Figs. 5 and 6. It is important to note that the thin electrolyte YSZ film appeared fully dense, without any noticeable pores. It is also evident that the colloidal spraying method for electrolyte deposition described above allows for excellent control over the film thickness to within ± 2 μ m for a 20- μ m-thick electrolyte film. The Ni-containing catalytic layers appeared sufficiently porous to support adequate fuel supply. Overall, the structure of the layered electrodes (the Fe₃₀Cr₆AT), anode support layer, and the LSCF cathode in Fig. 6a and b appear to be sufficiently porous, and thus overpotentials due to mass transport could be expected to be relatively low during operation of the fuel cells.

3.3. Thermal cycling

To evaluate the effects of thermal cycling, the Fe₃₀Cr₃AT-supported fuel cell membranes were cycled 50 times between 475 and 1075 K, in 4% H₂/nitrogen at heating and cooling rates of approximately 50 K/min. The sealing material could develop some cracks during this process, and therefore thermally cycled SOFCs were resealed by the procedure described above prior to electrochemical testing. SEM images showed no cracking or

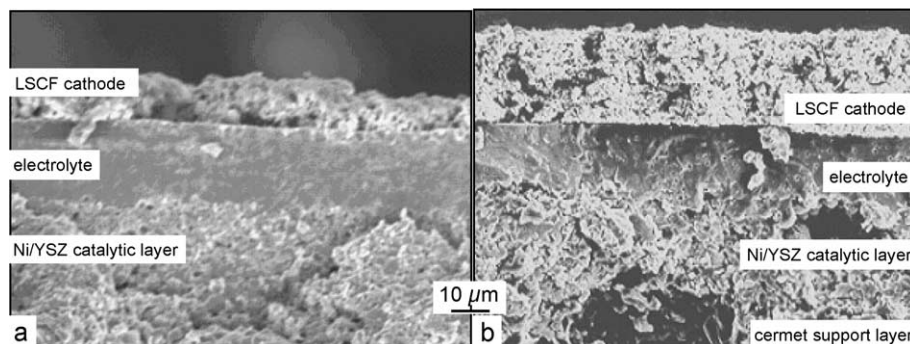


Fig. 6. (a) Fracture cross-section of a complete Fe₃₀Cr₃AT-supported SOFC membrane after firing at 1575 K before thermal cycling. (b) Fracture cross-section of a complete Fe₃₀Cr₃AT-supported SOFC membrane after 50 rapid thermal cycles (between 475 and 1075 K) and electrochemical testing.

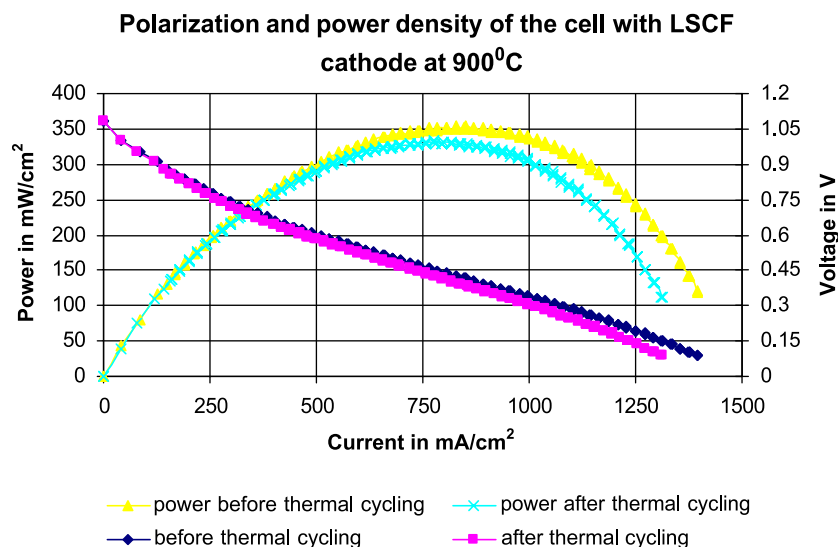


Fig. 7. Power density and polarization of the Fe₃₀Cr₃AT-supported fuel cell with LSCF cathode before and after thermal cycling at 1175 K (900 °C).

delamination of the multilayer SOFC membranes themselves, following the rapid thermal cycling, as is also evident in Fig. 6a and b.

3.4. Current/voltage (*I*–*V*) testing of the fuel cell membranes

Typical *I*–*V* curves for the membranes before and after thermal cycling are shown in Fig. 7. Performance data in Fig. 7 labeled ‘before and after thermal cycling’ refer to the cells tested before and after 50 rapid thermal cycles. It is clear that the thermal cycling affected only minimally the performance of these cells. At 1175 K, both samples show a maximum power density of about 3500 W/m² (350 mW/cm²), with similar *I*–*V* responses. The use of a better cathode catalyst would likely improve cell performance. These results indicate that the close thermal expansion matching of porous metal cermet support electrodes to that of the zirconia electrolyte can be successful in eliminating the deleterious effects of rapid thermal cycling on SOFC membrane performance.

4. Conclusions

SOFC membranes were prepared, in which the thin zirconia electrolyte film is supported by a porous ferritic alloy layer of which the thermal expansion coefficient has been manipulated by the addition of 3 wt.% (6 vol.%) aluminum titanate. The compatibility of the various membrane layers during the processing has been shown. The ability of the cermet-supported thin film SOFC membranes to withstand rapid thermal cycling between 475 and 1075 K at 50 K/min has been demonstrated. Testing of the SOFC membranes in laboratory cells showed a peak power density of 3500 W/m² (350 mW/cm²) at 1175 K.

Acknowledgment

The authors gratefully acknowledge the experimental assistance of Dr. I. Villareal (Ikerlan Technological Research Center, Álava, Spain) and of D. Blum. Dr. I. Stephan is thanked for useful discussions.

The support for this work was provided by the California Energy Commission, Pier-EISG program, with additional support from the U.S. Department of Energy, Fossil Fuel Office-NETL.

References

- [1] A.V. Virkar, F. Kuan-Zong, S.C. Singhal, Paper Presented at the Proceedings of the Third International Symposium on Ionic and Mixed Conducting Ceramics, Electrochem. Soc., Pennington, NJ, USA, 1998, pp. 113–124.
- [2] S. De Souza, S.J. Visco, L.C. De Jonghe, *Solid State Ionics* 98 (1997) 57.
- [3] V. Agarwal, L. Meilin, *Journal of the Electrochemical Society* 143 (1996) 3239.
- [4] E. Schuller, R. Vassen, D. Stover, *Advanced Engineering Materials* 4 (2002) 659.
- [5] W. Bai, K.L. Choy, R.A. Rudkin, B.C.H. Steele, *Solid State Ionics* 113–115 (1998) 259.
- [6] S.A. Barnett, *Energy* 15 (1990) 1.
- [7] C.H. Wang, W.L. Worrell, S. Park, J.M. Vohs, R.J. Gorte, *Journal of the Electrochemical Society* 148 (2001) A864.
- [8] W. Bai, K.L. Choy, R.A. Rudkin, B.C.H. Steele, *Solid State Ionics* 115 (1998) 259.
- [9] N.Q. Minh, et al., Paper Presented at the Proceedings of the Third International Symposium on Solid Oxide Fuel Cells, Electrochem. Soc., Pennington, NJ, USA, 1993, pp. 801–808.
- [10] S. Linderoth, P.H. Larsen, Paper Presented at the New Materials for Batteries and Fuel Cells. Symposium (Materials Research Society Symposium Proceedings), *Mater. Res. Soc.*, vol. 575, 2000, pp. 325–330.

- [11] W. Glatz, et al., Paper Presented at the Solid Oxide Fuel Cells (SOFC VI), Proceedings of the Sixth International Symposium, Electrochem. Soc., Pennington, NJ, USA, 1999, pp. 783–790.
- [12] S. Visco, et al., Paper Presented at the Ionic and Mixed Conducting Ceramics IV, San Francisco, 2001.
- [13] I. Villarreal, et al., *Electrochemical and Solid-State Letters* 6 (2003) A178.
- [14] N.Q. Minh, Paper Presented at the Proceedings of the Fourth International Symposium on Solid Oxide Fuel Cells (SOFC-IV), Electrochem. Soc., Pennington, NJ, USA, 1995, pp. 138–145.
- [15] S.C. Singhal, Paper Presented at the High Temperature Electrochemistry: Ceramics and Metals. Proceedings of the 17th Riso International Symposium on Materials Science. Riso Nat. Lab., Roskilde, Denmark, 1996, pp. 123–138.
- [16] A.C. Muller, D. Herbstritt, E. Ivers-Tiffée, *Solid State Ionics* 152–153 (2002) 537.
- [17] G. Tilloca, *Journal of Materials Science* 26 (1991) 2809.
- [18] D.S. Perera, D.J. Cassidy, *Journal of Materials Science Letters* 16 (1997) 699.
- [19] H.A.J. Thomas, R. Stevens, *British Ceramic Transactions and Journal* 88 (1989) 144.
- [20] L.A. Chick, et al., *Materials Letters* 10 (1990) 6.